

## Ground effect for low-frequency noise

Remigiusz PYFFEL , Maciej BUSZKIEWICZ , Roman GOŁĘBIEWSKI 

Department of Acoustics, Adam Mickiewicz University, Uniwersytetu Poznańskiego 2, 61 – 614 Poznań

**Corresponding author:** Roman GOŁĘBIEWSKI, email: roman.golebiewski@amu.edu.pl

**Abstract** Low-frequency noise is an environmental concern, as it is poorly attenuated by buildings and atmospheric conditions, allowing it to propagate over long distances and affect human well-being. It is emitted by sources such as vehicles, wind turbines, and industry, and is often underestimated by standard A-weighting. Noise propagation in open space is significantly influenced by the ground effect. This phenomenon involves the interference between direct and ground-reflected sound waves, determined by the ground's finite acoustic impedance, characterized by the effective flow resistivity,  $\sigma$ . At very low frequencies, this interaction often results in constructive interference and increased sound pressure levels. This research aimed to verify a calculation model for accurately predicting low-frequency sound pressure levels, specifically considering the ground interaction. The study involved measuring single vehicle pass-by noise at two distances from a road: 7.5m and 50m. Sound power levels of the vehicles were determined from measurements taken closer to the road (7.5m). The effective flow resistivity,  $\sigma$ , of the ground was estimated by comparing maximum sound levels measured at the two points with model predictions for different  $\sigma$  values. Using the estimated  $\sigma$  value and the calculated sound power levels, noise exposure levels at the 50m point were predicted using the ground interaction model and compared with the measured values. The results showed good agreement between calculated and measured noise exposure levels, particularly for low frequencies. Larger differences observed at medium and high frequencies were attributed to atmospheric turbulence, which has a less significant impact on low frequencies due to their larger wavelengths. The study concluded that the utilized model allows for accurate prediction of noise levels at a greater distance from the source, especially in the low-frequency range, by correctly modelling the acoustic interaction with the ground surface.

**Keywords:** ground effect.

### 1. Introduction

Noise propagation in open space depends on many phenomena. Close to the source, geometrical spreading and ground effect have a major influence on noise propagation. Further from the source, air absorption, refraction and the atmospheric turbulence must be taken into consideration [1].

The ground effect phenomenon involves the interference of a direct wave and a reflected wave from the ground surface. This phenomenon is caused by the finite impedance of the ground, which causes the amplitude and phase of the reflected sound to fluctuate as a function of frequency [2]. Interference can be constructive or destructive, depending on the phase difference between the direct and reflected paths [3]. At very low frequencies, the phase difference between the direct and reflected wave, especially over soft ground, is small. This leads to constructive interference, resulting in an increase in sound pressure level compared to propagation in free space. Surface reflection can increase sound pressure levels by as much as +6 dB. Constructive and destructive interference occur alternately – as the frequency increases [3].

The interaction of an acoustic wave with the ground surface is particularly important when the source and observation point are close to the ground surface. For such cases, we can significantly affect the noise level at the observation point through the type of ground surface (between the source and observation point). Depending on the type of ground surface and the geometry of the source – observation point (the height of the source and observation point and the distance from the source) the value of the noise level can vary up to several decibels.

There are many models describing the interaction of an acoustic wave with the ground surface. These models take into account the properties of the ground surface described by the so-called effective flow resistivity,  $\sigma$ . Soft surfaces (e.g., grass, arable soil, dense vegetation, soft snow) have high porosity and lower effective flow resistance. Harder surfaces (e.g., concrete, asphalt, water, ice, compacted earth, rock) have

low porosity and low effective flow resistance [3]. For example, "road" can have a value of  $\sigma = 200 - 300$  [kPa · s/m<sup>2</sup>], and "leaf litter"  $\sigma = 20 - 30$  [kPa · s/m<sup>2</sup>].

There are also a number of empirical models commonly referred to as engineering models that describe the interaction of noise with the ground surface. These include, among others: ISO 9613 [4], CONCAVE, CNOSSOS-EU, Nord 2000 [2, 3, 5, 6]. However, it should be noted that empirical methods have some limitations, especially for low source heights above soft surfaces [3]. ISO 9613-2 uses the G (Ground factor) parameter to quantify the effect of the substrate, where  $G = 1$  for soft substrate,  $G = 0$  for hard substrate, and  $G = 0.5$  for mixed substrate. Octave-band attenuation calculations are based on empirical formulas that depend on substrate type and height. Empirical models (such as ISO 9613-2 and CONCAVE) may differ in their predictions from analytical models (such as Nord2000, CNOSSOS-EU, ENM), especially over soft surfaces, with ISO 9613-2 based on data from favourable conditions and CONCAVE based on neutral conditions [7].

For environmental noise sources, frequency correction A is applied [8]. The A-weighting correction curve primarily reduces the low-frequency range and, to a small extent, the high-frequency range. This causes low frequencies to be overlooked in the prediction of noise in the outdoor environment. Low frequencies (20-200 Hz) [9] are emitted by many sources, including heavy vehicles (often maxima around 63 Hz) [10] and large wind turbines, for which the low-frequency content increases with turbine size [11]. Sources of low-frequency noise also include moving trains – especially railroad sleepers [12] and industrial sources of all kinds. Despite being less audible at low levels, low frequencies have a high irritant potential and are poorly attenuated by building structures. They can cause sleep disturbances, affect concentration, and are often underestimated by A-weighting [9]. The pulsatile nature or fluctuation of sound levels at low frequencies (e.g., in the 0.5-4 Hz range) can significantly increase irritability (by 10-12 dB) [9].

It is also worth noting that the World Health Organisation classifies low-frequency noise (LFN) as an environmental problem that has various health impacts [13]. The significant contribution of spectral components in low frequencies can mean harmful effects on the human body and well-being [14, 15]. According to the literature [16] low-frequency noise has a significant impact on human hearing and well-being. It is therefore a mistake to exclude it from environmental noise assessments. It should also be noted that low-frequency noise is attenuated to a smaller extent than higher frequencies by the atmosphere and is less effectively screened by obstacles (e.g. noise barriers, buildings). This makes this noise propagate over long distances. Noise dominated by low frequencies can cause not only vibration of building elements, but also resonance in parts of the human body. In the presence of this type of noise, there is also a decrease in speech intelligibility. This is due to the effect of masking with low-frequency components, the range of the spectrum in which speech occurs (the so-called upward spread of masking) [17,18].

The purpose of the research presented in this paper was to answer the question of whether, using the so-called accurate model for calculating the impact of interaction with the ground surface, it is possible to reliably determine the value of sound pressure levels at low frequencies. For this purpose, the model used was described for a stationary point and moving noise sources. Car noise measurements (for single car trips) were then made at two different distances from the road. On the basis of the measurements taken close to the road, the values of the sound power level were determined, and then – using the presented model – the noise exposure level at a distance of 50 m from the road was calculated and compared with the values determined from the acoustic measurements. On the basis of the measurements and calculations, it can be concluded that the utilized model of acoustic wave interaction with the ground surface allows accurate prediction of noise levels at a greater distance from the road.

## 2. Noise of the stationary source above the ground surface

Let's consider a non-directional point source at the height  $H_s$  above a flat ground surface. The squared sound pressure in the  $n$ -th frequency band can be written as follows (for  $H_s$  and  $H_o \ll d$ ):

$$\langle p_n \rangle^2 = \frac{W_n \rho c}{4\pi d^2} G_n(d, H_s, H_o, f_n, Z_n), \quad (1)$$

where  $W_n$  is the sound power in the  $n$ -th frequency band,  $\rho c$  is the air specific impedance, and  $d$  is the distance between the source and the receiver. The ground factor  $G_n$ , describing the interaction between the sound wave and the ground surface, depends on the frequency  $f_n$ , the ground impedance in the  $n$ -th frequency band  $Z_n$ , and the height of the source  $H_s$  and the receiver  $H_o$  (Fig. 1).

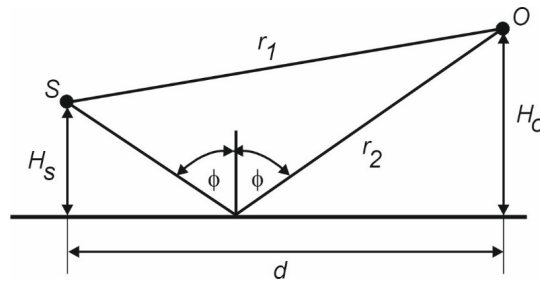


**Figure 1.** Source – receiver geometry in the horizontal plane.

In the simplest case, the ground impedance depends upon the effective flow resistivity,  $\sigma$  [19]:

$$Z_n = 1 + 9.08 \left(\frac{f}{\sigma}\right)^{-0.75} + i \cdot 11.9 \left(\frac{f}{\sigma}\right)^{-0.73} \quad (2)$$

Other models of ground impedance also exist [20].

The exact formula of the ground factor  $G_n$  is defined by [21],

$$G_n = 1 + |Q_n|^2 \left(\frac{r_1}{r_2}\right)^2 + 2|Q_n| \left(\frac{r_1}{r_2}\right) \cos\left(\frac{2\pi f_n}{c}(r_1 - r_2) + \varphi_n\right), \quad (3)$$

where  $r_1$ , and  $r_2$  denote the path lengths of the direct and the reflected wave (Fig. 1), and  $Q = Q \exp(i\varphi)$  is the complex, spherical wave reflection coefficient given by:

$$Q = R_p + (1 - R_p)F(\mu). \quad (4)$$

In the above equation,

$$R_p = \frac{\cos(\theta) - \frac{\rho_o c}{Z}}{\cos(\theta) + \frac{\rho_o c}{Z}} \quad (5)$$

is the plane wave reflection coefficient, and  $\theta$  is the reflection angle from the ground surface. The function  $F(\mu)$  is connected with the wave surface curvature.

Using the definition of sound pressure level,

$$L_{pn} = 10 \log\left(\frac{p_n^2}{p_o^2}\right), \quad p_o = 2 \cdot 10^{-5} Pa \quad (6)$$

and eq. (1), we obtain:

$$L_{pn} = L_{Wn} + 10 \log\left(\frac{S_o}{4\pi d^2}\right) + F_{gn}, \quad (7)$$

where the function

$$F_{gn} = 10 \log(G_n(d, H_s, H_o, f_n, Z_n)), \quad (8)$$

corresponds to the exact ground factor in decibels in the  $n$ -th frequency band.

In eq. (7):

$$L_{Wn} = 10 \log\left(\frac{W_n \rho c}{p_o^2 S_o}\right), \quad S_o = 1 m^2, \quad (9)$$

is the sound power level of the point source in the  $n$ -th frequency band.

If the effective flow resistivity  $\sigma$  is known, the quantity  $F_{gn}$  can be calculated at different distances and heights of the source and receiver.

The next few figures show the values of the  $F_{gn}$  function, for several specific source-receiver geometries and over different ground surfaces. As can be seen from the presented relationships, the  $F_{gn}$  function depends very strongly on the frequency and the source-observation point geometry. For low frequencies, reflection from the ground surface amplifies the amplitude of the acoustic wave – regardless of the type of ground surface and distance. For the middle range of frequencies, we observe the amplification and weakening of the amplitude of the acoustic wave depending on the frequency.

For acoustic soft ground (i.e. ground covered by grass) the value of the effective flow resistivity is low and the attenuation by the ground occurs at medium frequencies. For acoustic hard ground (i.e. concrete, water) the attenuation by the ground occurs at higher frequencies. The ground effect strongly depends on the height of the source and the receiver. When source or receiver is located close to the ground, the acoustic wave interaction with the ground surface effect strongly affects the noise amplitude. High above the surface, the phenomenon is less significant (Fig. 2 – 3).

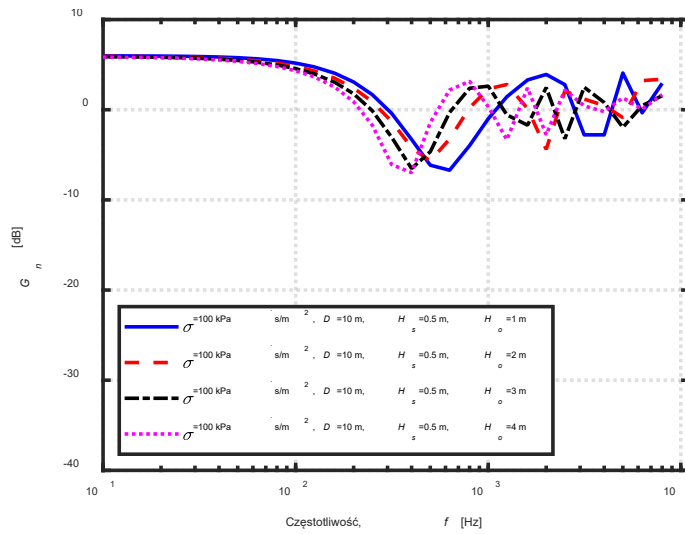


**Figure 2.** The fluctuations of  $F_{gn}$  as a function of frequency (eq. (3)) at the distance of 10m for  $\sigma = 100$  kPa·s/m<sup>2</sup>, for four different observation points ( $H_o = 1, 2, 3$  and 4 m).

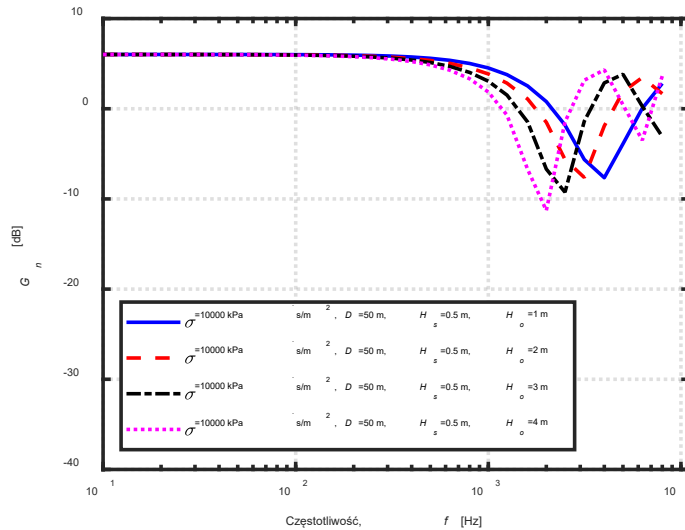


**Figure 3.** The fluctuations of  $F_{gn}$  as a function of frequency (eq. (3)) at the distance 50m for  $\sigma = 10000$  kPa·s/m<sup>2</sup>, at four different observation points ( $H_o = 1, 2, 3$  and 4 m).

Equation (1) describes the sound pressure in  $n$ -th frequency band. Let's consider the total sound pressure:

$$\langle p^2 \rangle = \sum_n \langle p_n^2 \rangle. \tag{10}$$

Using eq. (1) we obtain:

$$\langle p^2 \rangle = \sum_n \frac{W_n \rho c}{4\pi d^2} G_n(d, H_s, H_o, f_n, Z_n). \tag{11}$$

After the transformation, this can be written as:

$$\langle p^2 \rangle = \frac{W \rho c}{4\pi d^2} \sum_n q_n G_n(d, H_s, H_o, f_n, Z_n), \tag{12}$$

where

$$q_n = \frac{W_n}{W}, \tag{13}$$

is the relative sound power spectrum of the point source and  $W$  is the total sound power.

Using the definition of the sound level

$$L_p = 10 \log \left( \frac{\langle p^2 \rangle}{p_0^2} \right), \tag{14}$$

we obtain:

$$L_p = L_W + 10 \log \left( \frac{S_0}{4\pi d^2} \right) + \Delta L_g, \quad (15)$$

where

$$L_W = 10 \log \left( \frac{W}{W_0} \right), \quad (16)$$

is the total sound power level of the point source.

In eq. (16) the quantity:

$$\Delta L_g = 10 \log \sum_n q_n G_n(d, H_s, H_o, f_n, Z_n), \quad (17)$$

describes the total exact ground factor in decibels. To calculate  $\Delta L_g$  we must know the relative sound power spectrum of the source,  $q_n$ , and the effective flow resistivity,  $\sigma$ .

### 3. Noise of the moving source above the ground surface

The moving vehicle can be modelled by an omnidirectional point source. For a moving point source located at a height  $H_s$ , the A-weighted squared sound pressure is:

$$\langle p_n \rangle^2 = \frac{W_n \rho c}{4\pi d^2} G_n(d, H_s, H_o, f_n, Z_n), \quad (18)$$

where  $d$  is the temporary distance between the source and the receiver (Fig. 4) and  $G_n$  is given by Eq. (3).

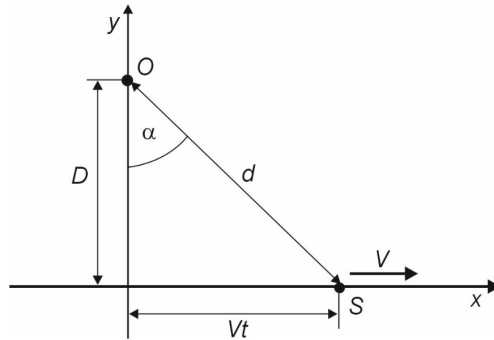


Figure 4. Source – receiver geometry.

The acoustic characteristics of the single noise event (e.g. a single vehicle’s pass-by) can be described by the sound exposure level defined as follows:

$$L_{En} = 10 \log \left( \frac{E_n}{E_o} \right), \quad (19)$$

where  $E_o = p_o^2 \cdot t_o$  ( $p_o = 2 \cdot 10^{-5}$  Pa,  $t_o = 1$  s) and  $E_n$  is the sound exposure in  $n$ -th frequency band defined by the equation:

$$E_n = \int_{-\infty}^{+\infty} \langle p_n^2(t) \rangle dt. \quad (20)$$

For a noise source moving at a steady speed ( $V = \text{const.}$ ), we can rewrite the above equation in the following form:

$$E_n = \frac{1}{V} \int_{-\infty}^{+\infty} \langle p_n^2(x) \rangle dx. \quad (21)$$

Using (eq. 18) we obtain:

$$E_n = \frac{1}{V} \int_{-\infty}^{+\infty} \frac{W_n \rho c}{4\pi d^2} G_n(d, H_s, H_o, f_n, Z_n) dx. \quad (22)$$

Using the dependences

$$\text{tg}(\alpha) = \frac{x}{D}, \quad (23)$$

and

$$d = \frac{D}{\cos(\alpha)}, \quad (24)$$

equation (22) takes the following form:

$$E_n = \frac{W_n \rho c}{4VD} \frac{1}{\pi} \int_{-\pi/2}^{+\pi/2} G_n(d(\alpha), H_s, H_o, f_n, Z_n) d\alpha. \quad (25)$$

Applying the definition of the sound exposure level (eq. 19), we obtain:

$$L_{En} = L_{Wn} + 10 \log \left( \frac{S_o}{4VDt_0} \right) + \Delta L_{Eng}, \quad (26)$$

where

$$L_{Wn} = 10 \log \left( \frac{W_n \rho c}{p_0^2 S_0} \right), \quad (27)$$

is the sound power level of a moving vehicle and

$$\Delta L_{Eng} = 10 \log(F_{ng}), \quad (28)$$

where

$$F_{ng} = \frac{1}{\pi} \int_{-\pi/2}^{+\pi/2} G_n(d(\alpha), H_s, H_o, f_n, Z_n) d\alpha. \quad (29)$$

Equation (26) allows us to calculate the noise exposure level for an omnidirectional point source moving at a constant speed,  $V$ , provided that the sound power level of the source and the effective flow resistivity,  $\sigma$ , are known.

#### 4. The measurements of traffic noise

To verify the model of the ground effect at low frequencies, measurements of single pass-by noise events were performed. The measurements were carried out near Poznan, on a road between two small villages: Kicin and Kliny.

Noise pressure levels were recorded at two different distances from the centre of the vehicle track:  $d_1 = 7.5$  m at the height  $H_o^{(1)} = 1.5$  m and  $d_2 = 50$  m - at the height  $H_o^{(2)} = 4.0$  m (Fig. 5).

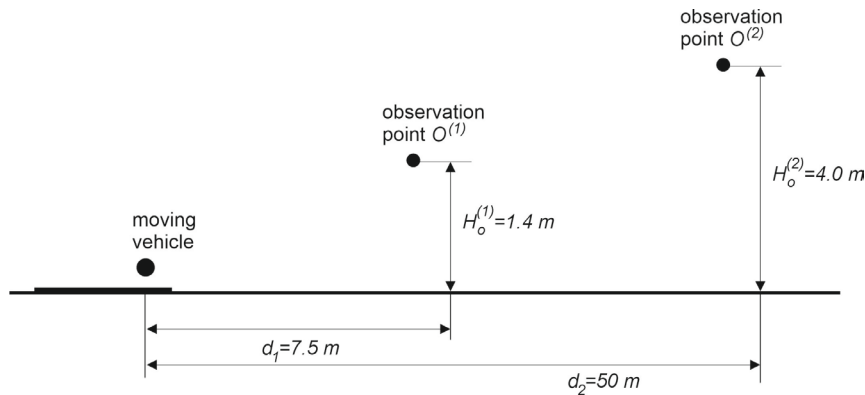


Figure 5. Location of the observation points.

During the measurements, the temporal variation in sound levels from single pass-by events was recorded in one-third octave frequency bands (in the frequency range of 0.8 Hz – 20 000 Hz). In addition, the speed of each vehicle was measured. During the measurements, a total of 207 moving light vehicles were recorded.

The ground between the source and the receivers: normal uncompacted ground. The weather conditions (temperature and humidity of air and wind speed and direction) were stable.

#### 5. The calculation of sound power level

Based on the recorded temporal changes of sound level in the one-third-octave frequency bands,  $L_{pn}(t)$ , the relative noise exposure was determined using the following equation:

$$E_n = \int_{-\infty}^{+\infty} 10^{0.1L_{pn}(t)} dt. \quad (30)$$

Using the determined relative noise exposure, the sound exposure level was calculated in the one-third octave frequency bands for each pass-by event. The following equation was used:

$$L_{En} = 10 \log(E_n). \tag{31}$$

Close to the source ( $D \rightarrow 0$ ) function  $F_{ng} \rightarrow 1$  (eq. (29)) and quantity  $\Delta L_{Eng} \rightarrow 0$ . It allows eq. (26) to be written in the following form:

$$L_{En} \cong L_{Wn} + 10 \log\left(\frac{S_o}{4VDt_o}\right). \tag{32}$$

To obtain the sound power level, the following relationship can be used:

$$L_{Wn} = L_{En} - 10 \log\left(\frac{S_o}{4VDt_o}\right). \tag{33}$$

The  $L_{En}$  values at the distance  $d_1 = 7.5$  m were used to determine the effective sound power level.

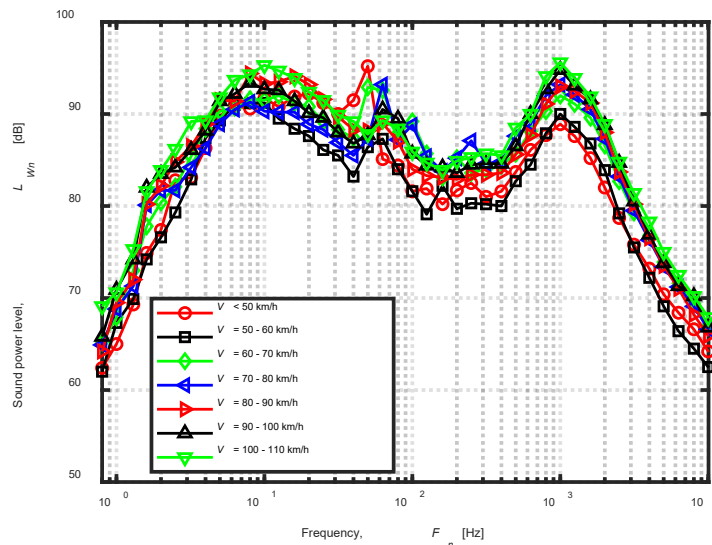


**Figure 6.** The sound power level of moving vehicles.

Using the obtained values of  $L_{Wn}$ , the sound exposure levels (for different vehicles moving at different velocities) at the distance  $d_2 = 50$  m were calculated (using eq. (26)) and then compared with the sound exposure levels obtained from field measurements.

To use formula (26) it is necessary to know the effective flow resistivity of the ground between the source and receiver. To determine the value of this parameter, we used the method described in the paper [22] adapted to the parameter  $L_{pmax}$  (chapter 6).

### 6. Estimation of the effective flow resistivity

As the vehicle moves, for  $d = D$ , the sound pressure level reaches its maximum value –  $L_p = L_{pmax}$ . With this in mind, we can use the sound pressure level relationships as for a stationary source.

Using eqs. (7) and (8) we can write the sound level for the first observation point (distance  $d_1$ , height  $H_o^{(1)}$ ):

$$L_{pmax}^{(1)} = L_W + 10 \log\left(\frac{S_o}{4\pi d_1^2}\right) + 10 \log\left(\sum_n q_n G_n^{(1)}(d_1, H_s, H_o^{(1)}, f_n, \sigma)\right), \tag{34}$$

and for the second observation point (distance  $d_2$ , height  $H_o^{(2)}$ ):

$$L_{pmax}^{(2)} = L_W + 10 \log\left(\frac{S_o}{4\pi d_2^2}\right) + 10 \log\left(\sum_n q_n G_n^{(2)}(d_2, H_s, H_o^{(2)}, f_n, \sigma)\right). \tag{35}$$

Subtracting the equations (34) and (35) we obtain:

$$L_{pmax}^{(1)} - L_{pmax}^{(2)} - 10 \log\left(\frac{d_2^2}{d_1^2}\right) = 10 \log\left(\frac{\sum_n q_n G_n^{(1)}(d_1, H_s, H_o^{(1)}, f_n, \sigma)}{\sum_n q_n G_n^{(2)}(d_2, H_s, H_o^{(2)}, f_n, \sigma)}\right). \tag{36}$$

Or, in the following equivalent form:

$$L_{pmax}^{(1)} - L_{pmax}^{(2)} - 10 \log \left( \frac{d_2^2}{d_1^2} \right) = 10 \log \left( \frac{\sum_n 10^{0.1(L_{Wn}-L_W)} G_n^{(1)}(d_1, H_s, H_o^{(1)}, f_n, \sigma)}{\sum_n 10^{0.1(L_{Wn}-L_W)} G_n^{(2)}(d_2, H_s, H_o^{(2)}, f_n, \sigma)} \right). \quad (37)$$

The correct value of the effective flow resistivity  $\sigma$  is obtained when the left,  $L$ , and right,  $R(\sigma)$ , sides of the above equation are equal. If there is no value of  $\sigma$  which makes  $L = R(\sigma)$ , then we use the value of  $\tilde{\sigma}$  which meets the condition:

$$|L - R(\tilde{\sigma})| = \min. \quad (38)$$

The value of effective flow resistivity was determined for each single pass-by event recorded simultaneously at both observation points.

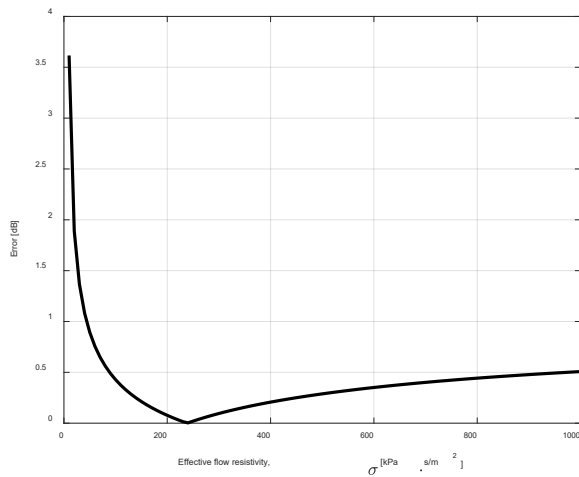


Figure 7. Numerical solution of eq. (36).

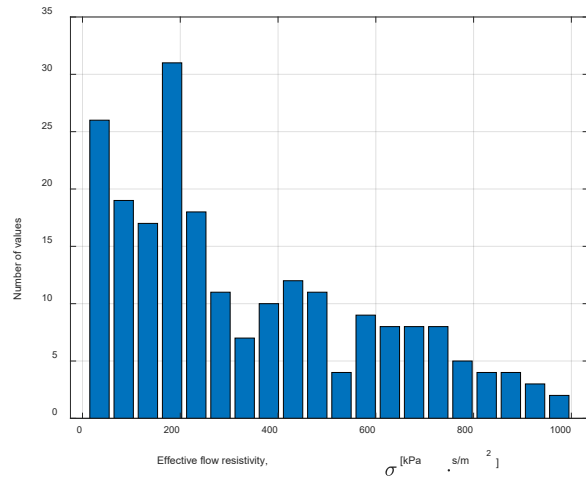


Figure 8. Histogram of the estimated values of effective flow resistivity.

The average value of flow resistance from all measurements was used in the subsequent acoustic calculations. The assumed value of this parameter equals  $\sigma = 340 \text{ [kPa} \cdot \text{s/m}^2\text{]}$ .

There are other methods for determining effective flow resistivity. For example, in the paper [23] a method for determining ground acoustic impedance was proposed. This method is based on two-channel measurements of the sound pressure level. The observation points should be located close to the ground and within a short distance from the source. In our measurements, the observation points were relatively far apart and second point (at the distance  $d_2 = 50 \text{ m}$ ) was located high above the ground surface ( $H_o^{(2)} = 4.0 \text{ m}$ ). In this situation, the weather conditions can influence the obtained results.

### 7. The calculation of sound exposure level

For each recorded pass-by, the sound power level was determined, and then the noise exposure level for the second observation point was calculated and compared with the value obtained from acoustic measurements. In the ground effect calculations, the average value of flow resistance determined in this paper was used.

Figure 9 presents the sound exposure levels measured and calculated at the distance  $d_2 = 50 \text{ m}$  and the height  $H_o^{(2)} = 4.0 \text{ m}$  for two speed ranges.

As can be seen, for low frequencies, there is good agreement between the calculated and measured values of noise exposure levels. Larger discrepancies are found for medium and high frequencies. These differences may be due to atmospheric turbulence, which affects the interaction between acoustic waves and the ground surface [22, 24]. The noise attenuation by the ground in turbulent atmospheric conditions is smaller than in non-turbulent conditions. Atmospheric turbulence has the greatest impact on the mid- and high-frequency range (about 500 Hz - 5 kHz), where it has the greatest impact on the propagation of acoustic waves, causing amplitude and phase instabilities. The impact is particularly strong for acoustic waves that are close to the scale of the turbulence (i.e., a few centimeters to a meter). For very low frequencies (<100 Hz) turbulence has less of an impact – the corresponding wavelengths (a few meters to several tens of meters) are much larger than typical turbulent structures.

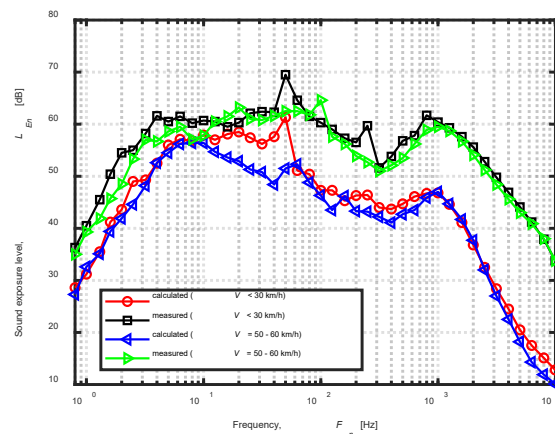


**Figure 9.** Comparison of the average measured and calculated sound exposure levels ( $d_2 = 50$  m,  $H_o^{(2)} = 4.0$  m).

## 8. Conclusions

Noise propagation in open spaces is complex, influenced by geometrical spreading, air absorption, refraction, atmospheric turbulence, and the ground effect. The ground effect is particularly significant near the source and receiver, involving interference between direct and ground-reflected sound waves. This interference, which can be constructive or destructive depending on phase differences, is caused by the finite impedance of the ground surface. At very low frequencies, the phase difference between direct and reflected waves is typically small, resulting in constructive interference and increased sound pressure levels, regardless of the ground type or distance. While attenuation over soft ground occurs at medium frequencies, hard ground causes attenuation at higher frequencies.

The study highlights the environmental impact of low-frequency noise, which is produced by sources including vehicles, large wind turbines, trains, and industrial facilities. Standard A-weighting often underestimates its effects. Low-frequency noise, even at levels below auditory thresholds, can be very annoying, disrupt sleep, impair concentration and performance, and – due to its pulsatile nature – can significantly increase irritability. Critically, low-frequency noise is poorly attenuated by typical building structures and atmospheric conditions, which allows it to propagate over long distances and cause vibrations in building elements or even resonance in the human body. It also decreases speech intelligibility through the upward spread of masking.

The research aimed to verify whether an "accurate model" for calculating the impact of ground interaction could reliably determine low-frequency sound pressure levels. The model treats noise sources as point sources (stationary or moving) and incorporates a ground factor dependent on frequency, ground impedance (related to effective flow resistivity,  $\sigma$ ), and geometry. Field measurements of single vehicle pass-by noise were performed at distances of 7.5 m and 50 m from a road. The 7.5m measurements were used to calculate the frequency-dependent sound power levels of the vehicles. The effective flow resistivity of the ground between the points was estimated by comparing the maximum measured sound pressure levels at the two distances with the values predicted by the model for different  $\sigma$  values. The average value of  $\sigma$ , along with the calculated sound power level, was then used in the model to predict sound exposure levels at the 50 m observation point.

Comparison of the calculated and measured sound exposure levels at 50 m showed good agreement, particularly for low frequencies. Larger differences were observed for medium and high frequencies. This discrepancy is attributed to atmospheric turbulence, which significantly affects acoustic wave propagation and ground interaction in the mid- and high-frequency ranges (around 500 Hz – 5 kHz), while having less impact on very low frequencies due to their much larger wavelengths compared to turbulent structures. The study concludes that the adopted model of acoustic wave interaction with the ground surface provides accurate predictions of noise levels at greater distances, particularly in the low-frequency range. This supports its utility for assessing environmental noise where the ground effect plays a major role.

## Additional information

The authors declare: no competing financial interests and that all material taken from other sources (including their own published works) is clearly cited and that appropriate permits are obtained.

## References

1. T. F. W. Embleton; Tutorial on sound propagation outdoors; *The Journal of the Acoustical Society of America*, 1996, 100(1), 31–48; DOI: 10.1121/1.415879
2. K. Attenborough; A comparison of engineering methods for predicting ground effect; *Forum Acusticum*, Berlin, 1999
3. N. Garg, S. Maji; A critical review of principal traffic noise models: Strategies and implications; *Environmental Impact Assessment Review*, 2014, 46, 68–81; DOI: 10.1016/j.eiar.2014.02.001
4. ISO 9613-2:2024; Acoustics — Attenuation of sound during propagation outdoors — Part 2: Engineering method for the prediction of sound pressure levels outdoors; 2024
5. K. Yamamoto, M. Yamashita, T. Mukai; Revised expression of vehicle noise propagation over ground; *J. Acoust. Soc. Jpn. (E)*, 1994, 15, 233–241
6. R. Gołębiewski, R. Makarewicz; Engineering formulas for ground effects on broad-band noise; *Applied Acoustics*, 2002, 63(9), 993–1001; DOI: 10.1016/S0003-682X(02)00007-5
7. L. Jenkin, J. Peng, J. Parnell; Comparison of five general noise prediction models and their performance in estimating low frequency noise propagation; *Annual Conference of the Australian Acoustical Society 2021 Making Waves AAS 2021*
8. IEC 61672-1:2013; Electroacoustics – Sound level meters – Part 1: Specifications; IEC, 2013
9. K. P. Waye; Effects of Low Frequency Noise and Vibrations: Environmental and Occupational Perspectives; *Encyclopedia of Environmental Health*, Elsevier, 2011, 2, 240–253; DOI: 10.1016/B978-0-444-52272-6.00245-2
10. G. Taraldsen, H. Jonasson; Aspects of ground effect modeling; *The Journal of the Acoustical Society of America*, 2011, 129(1), 47–53; DOI: 10.1121/1.3500694
11. C. S. Pedersen, H. Møller; An analysis of low frequency noise from large wind turbines; *Proceedings of the 14th International Meeting on Low Frequency Noise and Vibration and Its Control*, 2010, 339–360
12. D. Thompson; Introduction to Rolling Noise; *Railway Noise and Vibration*, Elsevier, 2009, 11–27; DOI: 10.1016/B978-0-08-045147-3.00002-5
13. World Health Organization Regional Office for Europe; Environmental noise guidelines for the European Region; WHO Regional Office for Europe, 2018
14. H. G. Leventhall; Low frequency noise and annoyance; *Noise Health*, 2004, 6(23), 59–72
15. N. Broner; The effects of low frequency noise on people - a review; *Journal of Sound and Vibration*, 1978, 58(4), 483–500
16. B. Berglund, P. Hassmén, R. F. S. Job; Sources and effects of low-frequency noise; *The Journal of the Acoustical Society of America*, 1996, 99(5), 2985–3002; DOI: 10.1121/1.414863
17. E. S. Martin, J. M. Pickett; Sensorineural Hearing Loss and Upward Spread of Masking; *Journal of Speech and Hearing Research*, 1970, 13(2), 426–437; DOI: 10.1044/jshr.1302.426
18. E. M. Danaher, J. M. Pickett; Some Masking Effects Produced by Low-Frequency Vowel Formants in Persons with Sensorineural Hearing Loss; *Journal of Speech and Hearing Research*, 1975, 18(2), 261–271; DOI: 10.1044/jshr.1802.261
19. M. E. Delany, E. N. Bazley; Acoustical properties of fibrous absorbent materials; *Applied Acoustics*, 1970, 3(2), 105–116; DOI: 10.1016/0003-682X(70)90031-9
20. K. Attenborough; Acoustical impedance models for outdoor ground surfaces; *Journal of Sound and Vibration*, 1985, 99(4), 521–544; DOI: 10.1016/0022-460X(85)90538-3
21. C. F. Chien, W. W. Soroka; A note on the calculation of sound propagation along an impedance surface; *Journal of Sound and Vibration*, 1980, 69(2), 340–343; DOI: 10.1016/0022-460X(80)90618-5
22. R. Gołębiewski; Simple methods for determination of the acoustical properties of ground surfaces; *Archives of Acoustics*, 2007, 32(4)
23. Report NT ACOU 104; Ground Surfaces: Determination of the Acoustic Impedance; Nordtest, 1999
24. R. Gołębiewski; Influence of turbulence on train noise; *Applied Acoustics*, 2016, 113, 39–44; DOI: 10.1016/j.apacoust.2016.06.003